SEISMIC BEHAVIOR OF CONCRETE BLOCK MASONRY PIERS

P.A. Hidalgo, R.L. Mayes, H.D. McNiven and R.W. Clough

SYNOPSIS

Experiments were conducted to evaluate the seismic resistance of window piers typical of high-rise concrete block masonry construction. Twenty-four fixed ended piers were subjected to cyclic, in-plane shear loads. Principal test parameters were the height-to-width ratio, the amount of vertical and horizontal reinforcement and the effect of full and partial grouting. Results include an identification of the principal modes of failure, the ultimate strength associated with the modes of failure and the effect of the test parameters on the ultimate strength. The results also include a discussion on the methods to predict the strength associated with each of the modes of failure and discussion of the inelastic characteristics of piers exhibiting the shear mode of failure. In particular, the effects of horizontal reinforcement and partial grouting on the shear mode of failure are presented.

RESUME

Vingt-quatre essais cycliques de charges latérales appliquées dans le plan de murs porteurs en blocs de ciment de construction en maçonnerie sont résumés. Les paramètres importants sont: la hauteur relative du mur, le montant d'armature verticale et horizontale, et l'effet d'avoir le mortier sur toute ou une partie des joints. Les modes de rupture ainsi que la résistance ultime pour les diverses combinaisons sont présentés.

Pedro A. Hidalgo obtained his Ph.D. from the University of California, Berkeley, in 1974. He is currently an Associate Research Engineer in the Earthquake Engineering Research Center (EERC) at the University of California, Berkeley.

Ronald L. Mayes obtained his Ph.D. from the University of Auckland, New Zealand, in 1972, and has worked as an Assistant Research Engineer at the EERC, University of California, Berkeley, for the past seven years. He has his own consulting practice firm, Computech, in Berkeley, and for the past two years has been the Technical Director of the Applied Technology Council.

Hugh D. McNiven obtained his Ph.D. from Columbia University in New York City in 1958. He is currently Professor of Engineering Science at the University of California in Berkeley and has been a faculty member of the Earthquake Engineering Research Center since 1972.

Ray W. Clough has been in the teaching staff of the University of California since 1949, and served as Director of the Earthquake Engineering Research Center for several years before taking his present position as Assistant Director in charge of the experimental research facilities.

INTRODUCTION

In determining the lateral load capacity of masonry piers and panels, the first step is to evaluate the mode of failure. Because most failures in past earthquakes have been characterized by diagonal cracks, many research programs have concentrated on this type of failure mechanism. Test techniques used by Blume (1), Greenley and Cattaneo (3), and others, induce the diagonal tension or shear mode of failure. Scrivener (12), Meli (9), Williams (13) and Priestley and Bridgeman (10) recognized that there were two possible modes of failure for cantilever piers. In addition to the shear or diagonal tension mode of failure, they recognized that for certain piers, a flexural failure could occur. This mechanism is characterized by yielding of the tension steel of the wall, followed by a secondary compressive failure at the toe,with associated buckling of the reinforcement once confinement is lost. Meli described the flexural failure as similar to that of an underreinforced concrete beam; i.e. with extensive flexural cracking and strength limited by yielding of the reinforcement with the failure finally due to crushing of the compressive corner or to rupture of the extreme bars.

Priestley (11) has performed several extensive series of tests on cantilever piers and has shown that very desirable inelastic behavior can be obtained with the flexural mode of failure. Consistent with this result, he has recommended that in the conceptual design of a building, all walls be designed to act as cantilever walls (Fig. 1) so that desirable inelastic structural behavior

is attained. It is clear that this may be a difficult architectural constraint, and consequently the inelastic behavior of walls other than cantilever walls must be investigated.

This paper presents the results obtained with full-scale, hollow concrete block piers, tested under cyclic lateral loads. The test fixture constrained the top and bottom sections against rotation, forcing the piers to deform in double curvature. The first seven tests reported here (piers with a height-to-width ratio of 2) were performed with a double pier specimen (Figs. 2 and 3), which closely represented the actual boundary conditions found in the perforated shear wall illustrated in Fig. 1. The cost of the double pier tests, both in money and time, precluded carrying out the rest of the test program using this test procedure, and consequently, a single pier test program was devised which greatly simplified the investigation (Fig. 4). The piers with height-to-width ratios of 1 (eleven tests) and 0.5 (six tests) were tested using the single pier test setup.

The double pier tests using a height-to-width ratio of 2 (labeled HCBL-21) were devised to investigate the effect of variations in bearing stress and horizontal and vertical reinforcement on the mode of failure and inelastic behavior. These tests showed that the flexural mode of failure in a fixed ended pier had desirable characteristics, however, these were not as desirable as those obtained by Priestley with cantilever piers. Furthermore, it was recognized that the amount of horizontal reinforcement used in Priestley's tests was substantially greater than that required by the current Uniform Building Code (UBC). This fact and the recognition that the flexural mode of failure is difficult to achieve in fixed ended piers with either a low height-to-width ratio or a significant compressive force due to the overturning moment effect, led to an investigation on the effects of lesser amounts of horizontal reinforcement on the shear mode of failure. The specific objective was to determine if desirable behavior could be obtained after major diagonal shear cracks occurred. The single pier tests with height-to-width ratios of 1 (HCBL-11) and 0.5 (HCBL-12) dealt with this effect. The partial grouting study was also included in the HCBL-11 tests.

TEST SPECIMENS

DOUBLE PIER SPECIMENS. The overall dimensions of the seven double pier test specimens were the same and are shown in Fig. 3. The test specimen was designed to satisfy as closely as possible the boundary conditions of piers in a real structure. The piers, which had a height of 5 ft. 4 in. and width of 2 ft. 8 in. were the elements of interest. The top and bottom spandrels were heavily reinforced (using No. 7 reinforcing bars as shown in Fig. 3) in an attempt to prevent their failure, although this objective was not achieved in all cases.

The panels were constructed from standard two-core reinforceable hollow concrete blocks, nominally 6 in. wide by 8 in. high by 16 in.

long. The core of each block had an area of approximately 51.4 sq. in. with a ratio of net (concrete) to gross (block) area of 58 percent. Both the piers and the top and bottom spandrel beams were fully grouted. The standard two-core reinforceable hollow concrete blocks, when tested as single units, had an average gross compressive strength of 1714 psi (2944 psi net strength). The average net tensile strength of the unit was 267 psi. The mortar was specified as standard ASTM Type M (i.e., 1 Cement: 1/4 Lime: 2-1/4 to 3 Sand), with a minimum strength of 2500 psi. The grout was also specified according to ASTM specifications. Because the panels were built at different times, the grout and mortar strength for each set varied according to normal workmanship.

The series of tests was planned to determine the effect of the bearing stress and the quantity of reinforcement on the strength and deformation properties of the piers, as shown in Table 1. Tests HCBL-21-13 and HCBL-21-15 had a substantial amount of horizontal reinforcement to ensure a flexural mode of failure while the rest of the specimens were expected to exhibit a shear mode of failure. In addition to the horizontal and vertical reinforcement, specimen HCBL-21-15 had steel plates inserted in the mortar joints at each of the three courses at the top and bottom of each pier (7).

SINGLE PIER SPECIMENS. The overall dimensions of the eleven HCBL-11 single pier test specimens were 4 ft. 8 in. high and 4 ft. wide (1.17 height-to-width ratio). The top and bottom flanges that transfer the loads from the loading beam and into the base were 8 in. high and 5 ft. 4 in. long. These flanges were fully grouted and contained shear keys to transfer the load to the specimen (2). In the case of the six HCBL-12 single pier test specimens, the overall dimensions were 3 ft. 4 in. high and 6 ft. 8 in. wide (height-to-width ratio of 0.5); the top and bottom flanges were 8 in. high and 8 ft. long.

The HCBL-11 and HCBL-12 specimens were constructed from standard two-core reinforceable hollow concrete blocks, nominally 8 in. wide by 8 in. high by 16 in. long. The net to gross cross-sectional area was 58%. In the HCBL-11 specimens, the average gross compressive strength was 1800 psi (3100 psi net) and the average net tensile strength was 293 psi. In the case of the HCBL-12 specimens, the average gross compressive strength was 1880 psi (3650 net) and the average net tensile strength was 221 psi. The mortar used in the single pier specimens was the standard ASTM Type M, and the grout was 1C:3S:2G, where G refers to 10 mm maximum size local gravel.

The variables of the single pier test specimens are listed in Table 1. The parameters for the HCBL-11 piers included the amount of both vertical and horizontal reinforcement and the type of grouting; four of the eleven piers were partially grouted, that is, only the cells and the bond beams containing reinforcement were grouted. The parameters for the HCBL-12 piers included the amount of horizontal reinforcement only; all of these piers were fully grouted.

TEST EQUIPMENT AND PROCEDURE

The test equipment shown in Figs. 2 and 4 permits lateral loads to be applied in the plane of the piers, using two displacement controlled actuators with a combined maximum capacity of 150 kip. In the case of the HCBL-12 piers, the lateral load capacity had to be increased to ensure failure of the piers, and a 450 kip actuator was used. A vertical load may be applied to the piers through the springs and rollers shown above the spandrel beam in Fig. 2 and above the lateral loading beam in Fig. 4. The Thomson Dual Roundway Bearings connecting the springs to the loading beams allow the piers to move freely with minimal friction force.

In the single pier test setup, the two hinged external steel columns restrain the rotation of the top of the pier, forcing it towards a condition of rotation fixity at the top and bottom, similar to that of the top and bottom spandrel in the double pier test setup. The disadvantage of this test procedure is that the vertical load acting on the pier could not be controlled during the test, and in fact, increased as the in-plane displacement of the test specimen increased. Consequently, all of the single piers had a significant compressive load acting with the ultimate shear load, as reported in the last two columns of Table 1.

The loading sequence for each test consisted of sets of three sinusoidal displacement cycles applied at a specified actuator displacement amplitude. The specified amplitude was gradually increased and followed a sequence that varied according to the height-to-width ratio of the piers. In the case of the HCBL-21 piers the specified amplitude followed the sequence at 0.02 in., 0.04 in., ... 0.08 in., 0.12 in.... 0.20 in., 0.25 in.... 0.50 in., 0.60 in.... 1.50 in.. This sequence was changed during the HCBL-11 pier tests to 0.02 in., 0.04 in., 0.08 in., 0.10 in., 0.12 in., 0.14 in., 0.16 in., 0.20 in., 0.25 in.... 0.60 in., 0.70 in.... 1.20 in.. Finally, the sequence for the piers with height-to-width ratio of 0.5 was 0.005 in., 0.010 in., 0.015 in., 0.020 in., 0.03 in., 0.04 in., 0.06 in., 0.08 in., 0.10 in., 0.14 in., 0.18 in. ... 0.30 in., 0.35 in.... 0.60 in., 0.70 in., 0.80 in..

TEST RESULTS

The results presented in Table 1 include listings of the maximum shear forces (and stresses) and the axial force (and stress) present in the pier at the time the maximum (peak) shear force was attained. It should be noted that in the double pier tests, (HCBL-21), the actual axial load of the piers varied as a function of the overturning moment resulting from the applied lateral force; the values indicated in the last two columns refer to the pier where a tensile axial force is imposed by the overturning moment effect, since this is the pier which has the larger critical tensile stress and is expected to fail first in the shear mode of failure. For the

single piers HCBL-11 and HCBL-12, the vertical compressive load generally increased as the input displacement increased and the value at ultimate was always larger than the initial bearing stress.

The test results also include the envelopes of the hysteresis loops for most tests (Figs. 5 to 8). The hysteresis envelopes are a plot of the absolute average of the maximum positive and negative forces and corresponding displacements, for each of the three cycles of loading at a given input displacement amplitude. The ultimate shear forces given in Table 1 are the average and peak values. The peak ultimate value is the maximum shear force obtained in any one cycle of loading. The average ultimate value is the maximum value obtained from the hysteresis envelope. This is always less than the peak value, but except for a few cases, it is within 90 percent of the peak value.

In evaluating the inelastic characteristics of the pier behavior, the hysteresis envelopes provide a good visual picture, however, they must be considered in conjunction with other parameters to fully evaluate the inelastic behavior. The other parameters include the energy dissipated per cycle, the ultimate strength, indicators of ductility, and comparisons of crack patterns at equal displacements. The usefulness of hysteresis envelopes is that they provide visual comparisons of ductility and ultimate strength; however, they give no indication of the energy dissipated per cycle. The hysteresis envelopes (average maximum force-deflection curves) are used as a frame of reference for the discussion of the test results. The question as to what consitutes desirable inelastic behavior has been discussed in Reference (7) in qualitative terms.

DISCUSSION OF THE TEST RESULTS

The discussion of the test results is presented in two sections; the first on the modes of failures observed and the prediction of the ultimate strength associated with each of them, and the second on the inelastic characteristics of the pier behavior.

MODES OF FAILURE

Identification of modes -- A flexural mode of failure was obtained in specimens HCBL-21-13 and HCBL-21-15. The mode was identified as flexural in the following way. The specimens had flexural (horizontal) cracks only and the ultimate strength of the pier was controlled by the tensile yielding strength of the vertical reinforcement. The final mechanism of failure was due to crushing at the compressive toe.

All of the single pier tests (HCBL-11 and HCBL-12) as well as HCBL-21-1, 3, 5, 7, 9, displayed a shear mode of failure. This mode was characterized by early flexural cracks at the toes of the pier which were later augmented by diagonal cracks that extend through a partial zone of the pier. As the horizontal load increased, large diagonal (X-cracks) formed when the diagonal tensile stress in the

pier reached the tensile strength capacity of the masonry. These large diagonal cracks usually coincided with the ultimate lateral load capacity of the piers. Significant strength degradation generally occurred after the ultimate capacity was attained as shown in Figs. 5, 6 and 7.

Specimens HCBL-12-4 and 5 developed a final failure mechanism and ultimate strength due to a combination of shear cracks and sliding along a path determined by these diagonal cracks and the top course of the pier, (a bell-shape path). As it is unlikely that a pier in a real building may develop this mode of failure, the hysteresis envelopes of these tests were not included in Fig. 7.

Specimen HCBL-11-6 displayed a combined shear and flexural mode of failure. For this mode yielding of the vertical reinforcement begins to develop, but as the vertical compressive load induced by the single pier test setup increases, the flexural moment capacity of the pier sections increases as the tension vertical reinforcement continues to yield. This effect enables the lateral load capacity of the pier to increase until the diagonal tensile stress reaches the tensile strength of the masonry and a shear failure develops (4,2).

Ultimate strength -- The ultimate strength of each pier is determined by the lesser of the lateral capacities associated with the flexural or the shear mode of failure.

The "flexural lateral load capacity" (lateral load capacity associated with the flexural mode of failure) is a function of the tensile yield strength of the vertical reinforcement, the axial load and the dimensions of the pier (8,4).

The "shear lateral load capacity" (lateral load capacity associated with the shear mode of failure) is limited by the strength of masonry in diagonal tension. The shear lateral load capacity of the piers (Table 3) is enhanced by the amount of horizontal reinforcement (specimens HCBL-21-7, HCBL-11-6 and HCBL-11-11). This shear lateral load capacity is also a function of the vertical axial load, since the stress field in the pier, dictating the magnitude of the maximum diagonal tension, is influenced both by the lateral load and the vertical load. Therefore, an increase in the compressive load will allow for an increase in the lateral load before the maximum diagonal tensile stress reaches the tensile stress capacity of the masonry. To see this, compare the average prism strength, shear lateral load capacity and axial stress at ultimate for specimens HCBL-21 and HCBL-11 in Tables 3 and 4.

The lateral load required to develop a major diagonal crack (shear crack strength in Tables 2, 3, 4 and 5) coincided with the maximum lateral load in the case of the HCBL-21 piers failing in shear, and all the HCBL-11 piers. However, in the piers with height-to-width ratio of 0.5 the lateral load continued to increase after the occurrence of the first major diagonal crack, as

illustrated in Fig. 7 and Table 2. In this case the first major diagonal crack did not extend over the full width of the pier, thus permitting the formation of a compressive toe and an increase of the tensile stress of the vertical reinforcement. The horizontal load continued to increase until a diagonal crack fully separated the top from the bottom part of the pier, with the subsequent drop in lateral load capacity.

Prediction of the ultimate strength -- The methods suggested by various authors for predicting the flexural lateral load capacity of a pier (5,8,11,12) are similar and reasonably accurate, and are based on methods commonly used for reinforced concrete flexural elements. If all of the tension steel is assumed to be yielding and the moment of the resultant of compressive forces around the extreme compressive fiber is neglected, the moment capacity of a section under an axial compressive force N is given by

$$M = \Sigma \; A_{si} f_y d_i + N \frac{d}{2}$$

where d_i is the distance between the vertical reinforcing bar with area A_{si} and the extreme compressive fiber, d is the width of the pier and f_y is the yield strength of the vertical reinforcement. If M_b and M_t denote the moment capacity of the bottom and top sections of a pier of height h, the flexural lateral load capacity of a pier is

$$P = \frac{1}{h} (M_t + M_b)$$

If special devices such as those described in References (7,10) are used to increase the compressive strength of the masonry, the ultimate strength of the vertical steel should be used instead of the yield strength, in the computation of the flexural lateral load capacity of the pier (8).

For the shear mode of failure the theoretical and empirical relationships used to date for predicting the shear strength (5) possess different degrees of accuracy and generally contain a significant amount of scatter when they are correlated with experimental results. Thus, consideration of a lower bound for determining the shear strength is necessary for design purposes.

Table 4 presents the average shear crack strength, (from Table 3), for each series of piers with a different height-to-width ratio. It is observed that this strength is not only a function of the unit material strengths and the prism compressive strength, but is also affected by the amount of horizontal reinforcement and the axial load acting on the pier. However, the influence of the horizontal reinforcement on the shear crack strength of masonry does not appear to be defined clearly enough to be taken into account for design purposes.

Table 5 shows the results of two methods used to predict the shear crack strength of masonry walls. The first method is presently employed by the Uniform Building Code and uses the prism compressive strength f'_m to predict the pier shear strength τ_s, based on the net cross-sectional area of the pier. The values of f'_m/τ_s and $\tau_s/\sqrt{f'_m}$ have been computed in the last two columns of Table 5. This method does not take into account the effect of reinforcement nor the effect of an axial stress on the shear strength of the piers. The consequences of these simplifications are clearly shown in Table 5.

The second method used to predict the shear strength is based on a square panel diagonal compression test (8). The square panel critical tensile strength was determined in a study made by Blume (1), who proposed the following expression

$$\sigma^{o}_{tcr} = -0.582 \frac{P}{A} - \frac{\sigma_c}{2} + \frac{1}{2}\sqrt{4.849\left(\frac{P}{A}\right)^2 + \sigma_c^2}$$

where P is the ultimate load, A is the side area of the panel and σ_c is the edge pressure. In the present investigation the square panel tests were performed with zero edge pressure and therefore

$$\sigma^{o}_{tcr} = 0.734 \frac{P}{\sqrt{2}A}$$

The pier critical diagonal tensile stress has been computed at the neutral axis of the pier sections, following the simple beam theory for a section under combined flexure, shear and axial force. If a parabolic distribution of shear stress over the cross section is assumed, the pier critical tensile strength is given by

$$\sigma_{tcr} = -\frac{\sigma_c}{2} + \sqrt{(1.5\,\tau)^2 + \left(\frac{\sigma_c}{2}\right)^2}$$

where σ_c corresponds to the axial compressive stress at the neutral axis and τ represents the average shear stress over the cross section.

In spite of the fact that the square panel test can be considered more sophisticated than the prism test, since it induces a diagonal tension failure of the masonry assemblage and includes the axial stress effect on the critical tensile strength, the prediction of the shear crack strength of the piers using the prism compressive strength gives more consistent results, particularly if the ratio $\tau_s/\sqrt{f'_m}$ is considered. A shear crack strength of $3.0\sqrt{f'_m}$ (psi), where f'_m is used in psi, appears to be a reasonable figure for fully grouted, concrete block masonry piers.

INELASTIC BEHAVIOR OF PIERS

Flexural mode of failure -- The inelastic behavior characteristics revealed by the hysteresis envelopes of specimens HCBL-21-13 and 15 (Fig. 5) are quite desirable and similar to the behavior of an elasto-plastic material. The use of the plates in the mortar joints of specimen HCBL-21-15 significantly improved the deformation capability of the pier and the desirability of the hysteresis envelope.

A similar inelastic behavior could have been obtained for specimen HCBL-11-6 (Fig. 6), if the compressive load had not increased with the lateral displacement of the pier (4,2).

Shear mode of failure -- In the following subsections the inelastic characteristics of piers exhibiting a shear mode of failure are discussed in connection with two of the parameters used in the test program: the amount of horizontal reinforcement and the type of grouting. In addition to these two variables, it is important to state that more desirable inelastic behavior was obtained with the more squat HCBL-12 piers when compared to the behavior of more slender piers HCBL-11 and HCBL-21. Both the strength and deformation capacity of the HCBL-12 piers were increased after the occurrence of the first major diagonal crack, whereas for the HCBL-11 and HCBL-21 piers significant strength degradation occurred after the formation of the diagonal cracks.

a) Effect of horizontal reinforcement. Table 3 presents the shear crack strength for all piers that displayed a shear mode of failure; (in the case of the HCBL-12 piers this is the strength associated with the formation of the first full major diagonal crack, not the ultimate strength). Figures 5, 6 and 7 show the corresponding hysteresis envelopes.

In the case of the HCBL-21 piers, the only specimen with horizontal reinforcement, (HCBL-21-7), had a higher ultimate strength and a more desirable hysteresis envelope than the specimens with no horizontal reinforcement. In the HCBL-11 piers, the shape of the hysteresis envelopes appears to be independent of the amount of horizontal reinforcement. However, the strength and deformation capacity of the piers is improved with the use of horizontal reinforcement although this trend is not consistent (see specimen HCBL-11-9). The same conclusions obtained for the HCBL-11 piers are valid at a less pronounced level for the HCBL-12 piers. It should also be noted that increasing amounts of horizontal reinforcement improved the crack pattern that developed in the piers (2,4).

Another conclusion that is clear from the hysteresis envelopes of the piers exhibiting a shear mode of failure, is the inability of the horizontal reinforcement to develop its full yield capacity, (indicated by $A_{hs} f_y$ in Table 3), after the formation of the first

major diagonal crack. Before the test series began the authors hypothesized that the strength degradation and inelastic characteristics of piers failing in shear may be controlled by the yield capacity $A_{hs}f_y$ of the horizontal reinforcement. However, this was not validated by the test results. The inelastic characteristics of the piers after major diagonal cracking occurred was not significantly improved with increasing amounts of horizontal reinforcement. This may in part be attributable to the width of the piers and/or the type of anchorage used in the tests. The effect of the type of anchorage will be further investigated in later tests.

b) Effect of partial grouting. The comparison between fully and partially grouted HCBL-11 piers is presented in Table 1 and Fig. 8. In comparing both the net strength and hysteresis envelopes of fully and partially grouted piers, partial grouting decreases the deformation capability of the piers but increases the net strength. These are offsetting effects on the desirability of the inelastic behavior of the piers and in the authors' opinion cause a slight decrease in the desirability of the inelastic behavior of partially grouted piers when compared to fully grouted piers. In the case of strength, the net ultimate shear stress of partially grouted piers is of the order of 20% higher than fully grouted piers. In terms of deformation capability, the fully grouted piers could withstand 20% greater lateral displacements at failure than partially grouted piers.

SUMMARY OF TEST RESULTS

1. Two principal modes of failure occur in a masonry pier, a flexural mode and a shear mode.

2. The flexural lateral load capacity is determined by the yield strength of the vertical reinforcement, by the axial load and by the height and width of the pier. The flexural lateral load capacity can be predicted reliably by current analytical methods.

3. The strength associated with the shear mode of failure is a function of the tensile strength of the masonry assemblage and is affected by the axial stress on the pier and the amount of horizontal reinforcement. Two methods were used to predict the shear capacity of the piers and the method currently used in the Uniform Building Code gave the best correlation.

4. The flexural mode of failure shows desirable inelastic characteristics. The shear mode of failure of piers with height-to-width ratios of 2 or 1 is generally brittle and the serviceability of the piers is lost with the formation of the first major diagonal shear crack. However, the strength and deformation capacity of piers with height-to-width ratio of 0.5 continues to increase after the first major diagonal crack occurs with a resultant improvement in the post-cracking behavior when compared to more slender piers.

5. The use of horizontal reinforcement generally improves the inelastic behavior of piers exhibiting a shear mode of failure. However, with horizontal reinforcement ratios up to 0.5%, the piers were not able to develop the lateral load capacity determined by the yield strength of the horizontal reinforcement.

6. Partial grouting decreases the deformation capacity and increases the net shear strength when compared to fully grouted pier tests. These offsetting effects cause a slight decrease in the desirability of the inelastic behavior of partially grouted piers.

ACKNOWLEDGEMENTS

The research reported in this paper has been jointly funded by the National Science Foundation, the Masonry Institute of America and the Concrete Masonry Association of California and Nevada. The sponsorship of these institutions is gratefully acknowledged. Many helpful suggestions have been made by members of the masonry industry, including Messrs. W. Dickey, J. Amrhein, L. Thompson, S. Beavers, D. Prebble, D. Wakefield, J. Tawresey and other members of technical committees of various masonry organizations. D. A. Sullivan Co. fabricated the pier specimens. Thanks are also due to the EERC laboratory staff headed by D. Steere and I. Van Asten.

REFERENCES

1. Blume, J. A. and Proulx, J., "Shear in Grouted Brick Masonry Wall Elements", Report to Western States Clay Products from J. A. Blume and Associates, 1968.

2. Chen, S-W. J., Hidalgo, P.A., Mayes, R.L., Clough, R.W., and McNiven, H. D., "Cyclic Loading Tests of Masonry Single Piers, Volume 2--Height to Width Ratio of 1", EERC Report No. 78/28, University of California, Berkeley, 1978.

3. Greenley, D.G. and Cattaneo, L.E., "The Effect of Edge Load on the Racking Strength of Clay Masonry", Proceedings, Second International Brick Masonry Conference, Stoke-on-Trent, 1970.

4. Hidalgo, P.A., Mayes, R.L., McNiven, H.D. and Clough, R.W., "Cyclic Loading Tests of Masonry Single Piers, Volume 1--Height to Width Ratio of 2", EERC Report No. 78/27, University of California, Berkeley, 1978.

5. Mayes, R.L. and Clough, R.W., "State-of-the-Art in Seismic Strength of Masonry--An Evaluation and Review", EERC Report No. 75-21, University of California, Berkeley, 1975.

6. Mayes, R.L., Omote, Y., Chen, S.W. and Clough, R.W., "Expected Performance of Uniform Building Code Designed Masonry Structures", EERC Report No. 76-7, University of California, Berkeley, 1976.

7. Mayes, R. L., Omote, Y. and Clough, R.W., "Cyclic Shear Tests of Masonry Piers, Volume I--Test Results", EERC Report No. 76-8, University of California, Berkeley, 1976.

8. Mayes, R.L., Omote, Y. and Clough, R.W., "Cyclic Shear Tests on Masonry Piers, Vol. II - Analysis of Test Results", Report No. EERC 76-16, University of California, Berkeley, 1976.

9. Meli, R., "Behaviour of Masonry Walls under Lateral Loads", Proceedings of the Fifth World Conference on Earthquake Engineering, Rome 1973.

10. Priestley, M.J.N. and Bridgeman, D.O., "Seismic Resistance of Brick Masonry Walls", Bulletin of the New Zealand National Society for Earthquake Engineering, Vol. 7, No. 4, 1974.

11. Priestley, M.J.N., "Seismic Resistance of Reinforced Concrete Masonry Shear Walls with High Steel Percentages", Bulletin of the New Zealand National Society for Earthquake Engineering, Vol. 10, No. 1, 1977.

12. Scrivener, J.C., "Concrete Masonry Wall Panel Tests with Predominant Flexural Effect", New Zealand Concrete Construction, 1966.

13. Williams, D.W., "Seismic Behaviour of Reinforced Masonry Shear Walls", Ph.D. Thesis, University of Canterbury, Christchurch, New Zealand, 1971.

TABLE 1.

GENERAL TEST RESULTS

(Gross cross sections: HCBL-21 = 180 in^2, HCBL-11 = 366 in^2, HCBL-12 = 610 in^2 Net cross section HCBL-11 = 220 in^2)

SPECIMEN	TEST FREQUENCY (cps)	GROUTING Full (F) Partial (P)	INITIAL* BEARING STRESS (psi)	VERTICAL REINFORCEMENT No. Bars	Yield Strength (ksi)	$P_v = \frac{A_{vs}}{A_g}$	HORIZONTAL REINFORCEMENT No. Bars	Yield Strength (ksi)	$P_h = \frac{A_{hs}}{A_g}$	$A_{hs}\ f_y$ (kip)	RATIO OF TOTAL AREA OF STEEL TO GROSS AREA OF WALL $P_v + P_h$	AVERAGE ULTIMATE SHEAR FORCE (kip)	AVERAGE ULTIMATE SHEAR STRESS* (psi)	PEAK ULTIMATE SHEAR FORCE (kip)	PEAK ULTIMATE SHEAR STRESS* (psi)	AXIAL VALUE AT ULTIMATE** FORCE (kip)	AXIAL VALUE AT ULTIMATE** STRESS* (psi)
HCBL-21- 1	0.02	F	250	4#6	79.0	0.0098	-	-	-	-	0.0098	24.0	133	26.0	144	-12.0	-67
- 3	0.02	F	125	4#4	54.1	0.0044	-	-	-	-	0.0044	26.0	144	27.3	152	+12.2	+68
- 5	0.02	F	0	4#6	78.1	0.0098	-	-	-	-	0.0098	18.5	103	20.5	114	+26.1	+145
- 7	0.02	F	250	4#6	78.1	0.0098	3#5	67.8	0.0052	63.1	0.0149	39.0	217	40.7	226	+ 6.7	+37
- 9	0.02	F	500	4#6	78.5	0.0098	-	-	-	-	0.0098	28.7	159	29.5	164	-52.6	-292
-13	0.02	F	125	4#4	50.8	0.0044	3#7 2#5	62.9	0.0134	152.2	0.0179	26.0	144	29.1	162	+14.4	+80
-15	0.02	F	125	4#4	51.8	0.0044	3#7 2#5 PL	64.0	0.0134	154.9	0.0179	33.6	187	35.2	196	+22.2	+123
HCBL-11- 1	1.5	F	55	-	-	-	-	-	-	-	-	45.2	123	49.5	135	-44.0	-120
- 2	1.5	P	91(55)	-	-	-	-	-	-	-	-	25.2	115(69)	26.3	120(72)	-42.2	-192(-115)
- 3	1.5	F	55	2#5	70.8	0.0017	-	-	-	-	0.0017	46.3	127	49.1	134	-25.1	-69
- 4	1.5	F	55	2#5	70.8	0.0017	1#5	47.9	0.0008	14.8	0.0025	60.3	165	62.7	171	-39.1	-107
- 5	1.5	P	91(55)	2#5	70.8	0.0017	1#5	47.9	0.0008	14.8	0.0025	46.8	213(128)	49.6	226(136)	-30.2	-137(-83)
- 6	1.5	F	55	2#5	70.8	0.0017	4#5	47.9	0.0034	59.4	0.0051	72.8	199	82.7	226	-52.7	-144
- 7	1.5	F	55	2#8	69.2	0.0043	-	-	-	-	0.0043	53.6	146	65.8	180	-33.3	-91
- 8	1.5	P	91(55)	2#8	69.2	0.0043	-	-	-	-	0.0043	36.8	167(101)	37.9	172(104)	-29.2	-133(-80)
- 9	1.5	F	55	2#8	69.2	0.0043	2#5	47.9	0.0017	29.7	0.0060	53.6	146	56.9	155	-41.9	-114
-10	1.5	P	91(55)	2#8	69.2	0.0043	2#5	47.9	0.0017	29.7	0.0060	48.7	222(133)	50.2	228(137)	-31.2	-142(-85)
-11	1.5	F	55	2#8	69.2	0.0043	4#6	73.9	0.0048	130.1	0.0091	84.5	231	87.7	240	-50.8	-139
HCBL-12- 1	0.02	F	52	3#7	80.3	0.0030	-	-	-	-	0.0030	189.1	310	200.3	328	-118.5	-194
- 2	0.02	F	52	3#7	80.3	0.0030	1#5	69.6	0.0005	21.6	0.0035	201.5	330	211.7	347	-122.0	-200
- 3	0.02	F	52	3#7	80.3	0.0030	2#5	69.6	0.0010	43.2	0.0040	242.5	398	251.4	412	-148.5	-243
- 4	0.02	F	52	3#7	80.3	0.0030	3#5	69.6	0.0015	64.7	0.0045	209.9	344	218.6	358	-129.4	-212
- 5	0.02	F	52	3#7	80.3	0.0030	4#5	69.6	0.0020	86.3	0.0050	220.2	361	228.0	374	-130.9	-215
- 6	0.02	F	52	3#7	80.3	0.0030	4#6	67.3	0.0029	118.4	0.0058	252.0	413	261.7	429	-143.0	-234

* Partially grouted pier stresses computed using net areas. Values in parenthesis indicate gross area stresses.

** Positive values indicate tension; negative values indicate compression. For the double pier tests (HCBL-21) these values correspond to the pier where a tensile axial force is imposed by the overturning moment effect.

TABLE 2

SHEAR CRACK STRENGTH AND ULTIMATE STRENGTH FOR PIERS WITH HEIGHT TO WIDTH RATIO OF 0.5

Specimen	Grouting Full(F)	Initial Bearing Stress (psi)	Vertical Reinforcement	Horizontal Reinforcement		Shear Crack Strength		Compressive Stress at Shear Crack (psi)	Peak Ultimate Shear		Compr. Stress at Ultimate (psi)	Peak Ult. Shear / Shear Crack Strength
			No.Bars	No.Bars	A_{hs} f_y (kip)	Force (kip)	Stress (psi)		Force (kip)	Stress (psi)		
HCBL-12-1	F	52	3#7	---	---	115.2	189	85	200.3	328	194	1.74
-2	F	52	3#7	1#5	21.6	118.9	195	74	211.7	347	200	1.78
-3	F	52	3#7	2#5	43.2	130.5	214	76	251.4	412	243	1.93
-4	F	52	3#7	3#5	64.7	159.1	261	127	218.6	358	212	1.37 *
-5	F	52	3#7	4#5	86.3	142.6	234	115	228.0	374	215	1.60 *
-6	F	52	3#7	4#6	118.4	140.9	231	86	261.7	429	234	1.86

* Piers HCBL-12-4 and HCBL-12-5 had a combined shear and sliding failure.

TABLE 3

SHEAR CRACK STRENGTH OF PIERS FAILING IN THE SHEAR MODE OF FAILURE

Specimen	Grouting Full (F)	Initial Bearing Stress (psi)	Vertical Reinforcement			Horizontal Reinforcement				Ratio of Total Area of Steel to Gross Area of Wall	Axial Stress at Shear Crack * (psi)	Shear Crack Strength	
			No. Bars	Yield Strength (ksi)	$p_v = \frac{A_{vs}}{A_g}$	No. Bars	Yield Strength (ksi)	$p_h = \frac{A_{hs}}{A_g}$	$A_{hs} f_y$ (kip)	$p_v + p_h$		Force (kip)	Stress (psi)
HCBL-21-1	F	250	4#6	79.0	0.0098	---	---	---	---	0.0098	- 67	26.0	144
-3	F	125	4#4	54.1	0.0044	---	---	---	---	0.0044	+ 68	27.3	152
-5	F	0	4#6	78.1	0.0098	---	---	---	---	0.0098	+145	20.5	114
-7	F	250	4#6	78.1	0.0098	3#5	67.8	0.0052	63.1	0.0149	+ 37	40.7	226
-9	F	500	4#6	78.5	0.0098	---	---	---	---	0.0098	-292	29.5	164
Average:											-22		160
HCBL-11-1	F	55	---	---	---	---	---	---	---	---	-120	49.5	135
-3	F	55	2#5	70.8	0.0017	---	---	---	---	0.0017	- 69	49.1	134
-4	F	55	2#5	70.8	0.0017	1#5	47.9	0.0008	14.8	0.0025	-107	62.7	171
-6	F	55	2#5	70.8	0.0017	4#5	47.9	0.0034	59.4	0.0051	-144	82.7	226
-7	F	55	2#8	69.2	0.0043	---	---	---	---	0.0043	- 91	65.8	180
-9	F	55	2#8	69.2	0.0043	2#5	47.9	0.0017	29.7	0.0060	-114	56.9	155
-11	F	55	2#8	69.2	0.0043	4#6	73.9	0.0048	130.1	0.0091	-139	87.7	240
Average:											-112		177
HCBL-12-1	F	52	3#7	80.3	0.0030	---	---	---	---	0.0030	- 85	115.2	189
-2	F	52	3#7	80.3	0.0030	1#5	69.6	0.0005	21.6	0.0035	- 74	118.9	195
-3	F	52	3#7	80.3	0.0030	2#5	69.6	0.0010	43.2	0.0040	- 76	130.5	214
-4	F	52	3#7	80.3	0.0030	3#5	69.6	0.0015	64.7	0.0045	-127	159.1	261
-5	F	52	3#7	80.3	0.0030	4#5	69.6	0.0020	86.3	0.0050	-115	142.6	234
-6	F	52	3#7	80.3	0.0030	4#6	67.3	0.0029	118.4	0.0058	- 86	140.9	231
Average:											-94		221

* Positive values indicate tensile stresses; negative values indicate compressive stresses. For the double pier tests (HCBL-21) these values correspond to the pier where a tensile axial force is imposed by the overturning moment effect.

TABLE 4

AVERAGE STRENGTH OF MASONRY COMPONENTS FOR PIERS FAILING IN THE SHEAR MODE OF FAILURE

Specimen	Concrete Block Compressive Strength (psi)	Mortar Compr. Strength (psi)	Grout Compr. Strength (psi)	Prism Compr. Strength (psi)	Pier Shear Strength (psi)
HCBL-21	1714	4676	4444	2521 *	160
HCBL-11	1800	2324	4643	1710 **	177
HCBL-12	1880	5530	3890	2988 **	221

* Based on a prism with height to thickness ratio of 6.7.

** Based on a prism with height to thickness ratio of 5.

TABLE 5

PREDICTION OF PIER SHEAR CRACK STRENGTH

Specimen	Prism Compressive Strength f'_m (psi)	Square Panel Tensile Strength σ^o_{tcr} (psi)	Pier Shear Crack Strength τ_s (psi)	Pier Axial Stress at Shear Crack $\sigma_c^{(1)}$ (psi)	Pier Crit. Tensile Strength σ_{tcr} (psi)	$\frac{\sigma^o_{tcr}}{\sigma_{tcr}}$	$\frac{f'_m}{\tau_s}$	$\frac{\tau_s}{\sqrt{f'_m}}$
HCBL-21-1	2432	320	144	-67	186	1.72	16.9	2.92
-3	2256	337	152	+68	264	1.28	14.8	3.20
-5	2592	280	114	+145	258	1.09	22.7	2.24
-7	2805	326	226	+37	358	0.91	12.4	4.27
-9	2519	244	164	-292	140	1.74	15.4	3.27
HCBL-11-1	1330	124	135	-120	151	0.82	9.9	3.70
-3	1833	137	134	-69	170	0.81	13.7	3.13
-4	1833	137	171	-107	209	0.65	10.7	3.99
-6	1833	135	226	-144	275	0.49	8.1	5.28
-7	1905	166	180	-91	228	0.73	10.6	4.12
-9	1905	166	156	-114	183	0.91	12.2	3.57
-11	1330	133	240	-139	297	0.45	5.5	6.58
HCBL-12-1	2988	330	189	-85	244	1.35	15.8	3.46
-2	2988	330	195	-74	258	1.28	15.3	3.57
-3	2988	330	214	-76	285	1.16	14.0	3.91
-4	2988	330	261	-127	333	0.99	11.4	4.77
-5	2988	330	234	-115	298	1.11	12.8	4.28
-6	2988	330	231	-86	306	1.08	12.9	4.23

(1) $\sigma_c > 0$ indicates tensile axial stress.
$\sigma < 0$ indicates compressive axial stress.

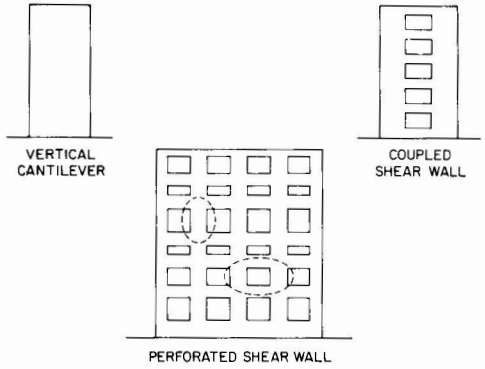

FIGURE 1 TYPICAL SHEAR WALLS

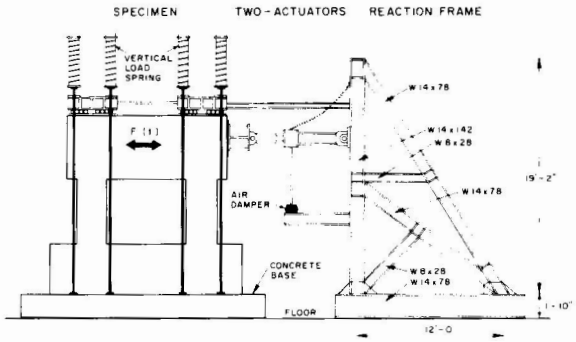

FIGURE 2 DOUBLE PIER TEST SET-UP

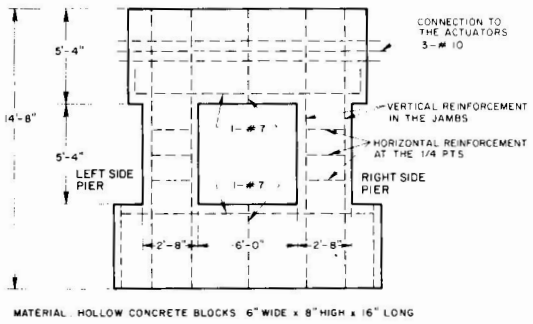

FIGURE 3 TYPICAL DOUBLE PIER TEST SPECIMEN

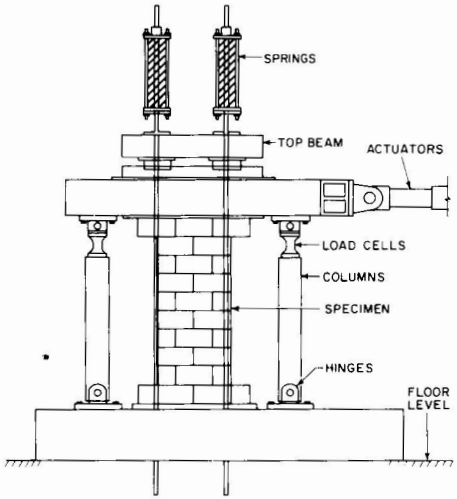

FIGURE 4 SINGLE PIER TEST SET-UP

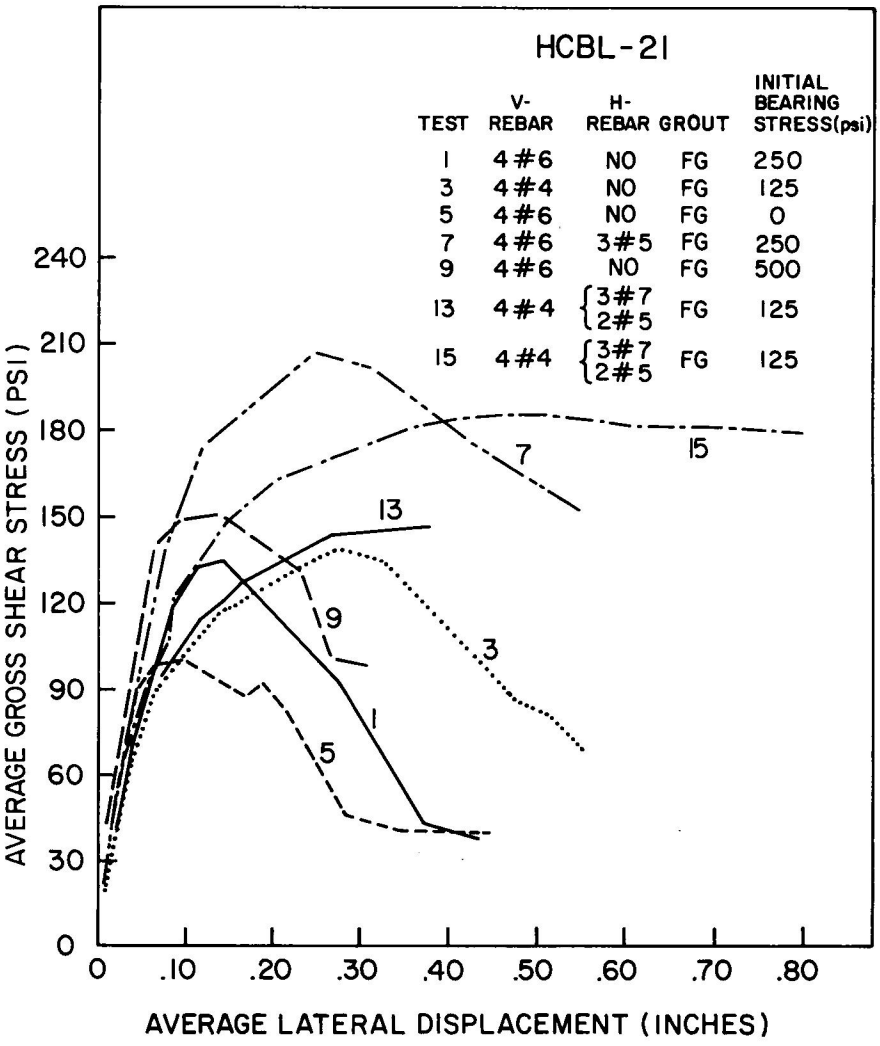

FIGURE 5. HYSTERESIS ENVELOPES FOR DOUBLE PIER TESTS (HCBL-21)

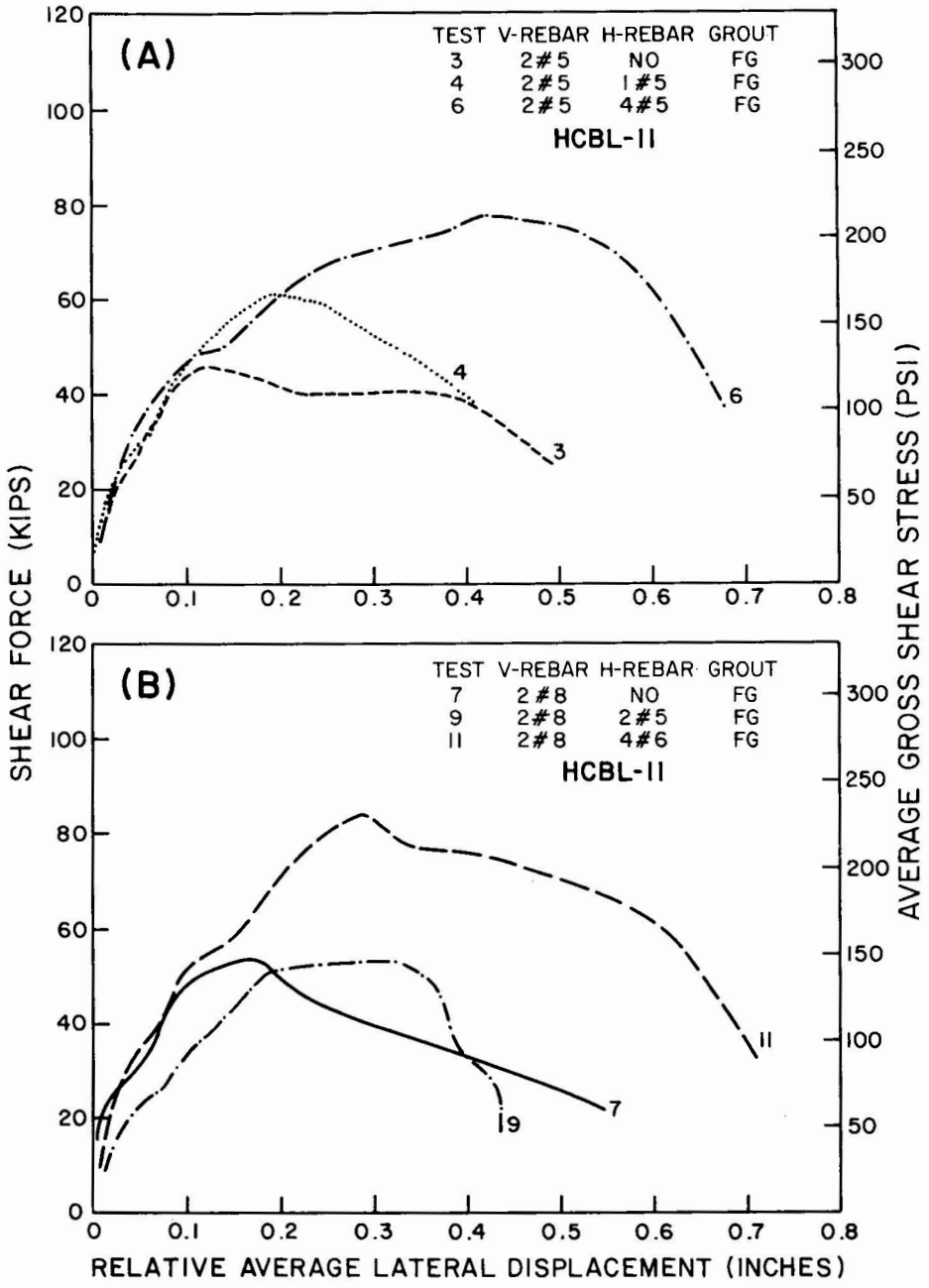

FIGURE 6. EFFECT OF REINFORCEMENT ON HYSTERESIS ENVELOPE. SINGLE PIER TESTS (HCBL-11)

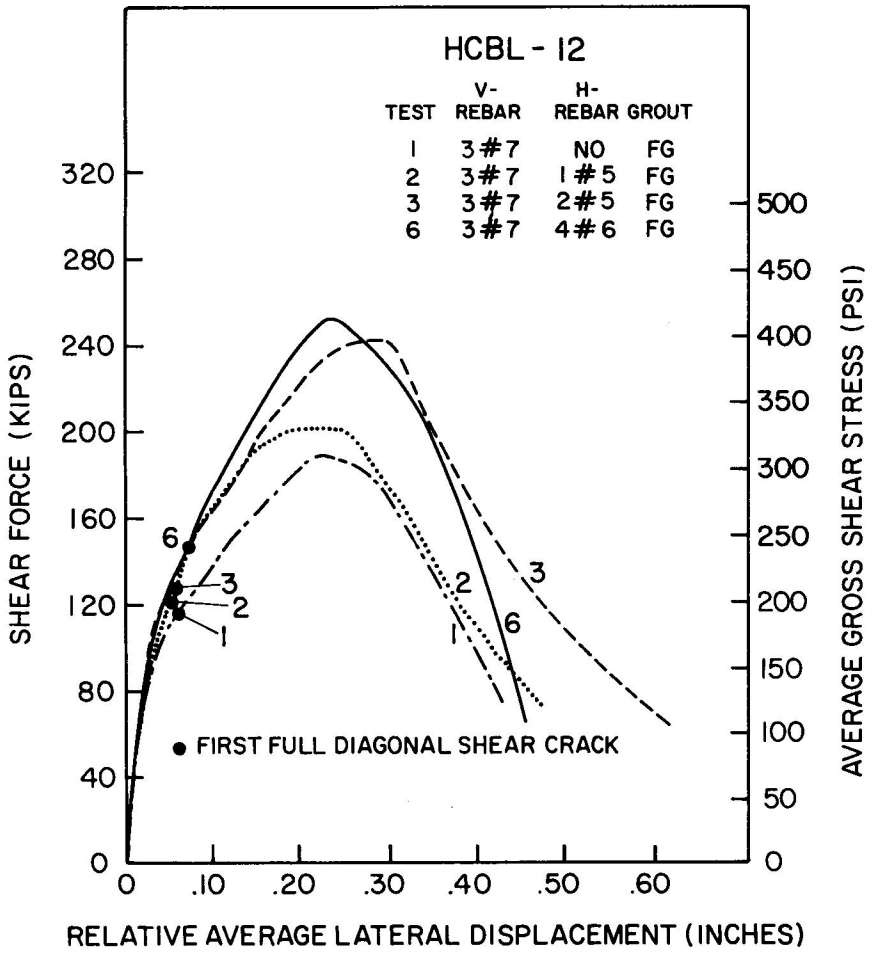

FIGURE 7. EFFECT OF HORIZONTAL REINFORCEMENT ON HYSTERESIS ENVELOPE. SINGLE PIER TESTS (HCBL-12)

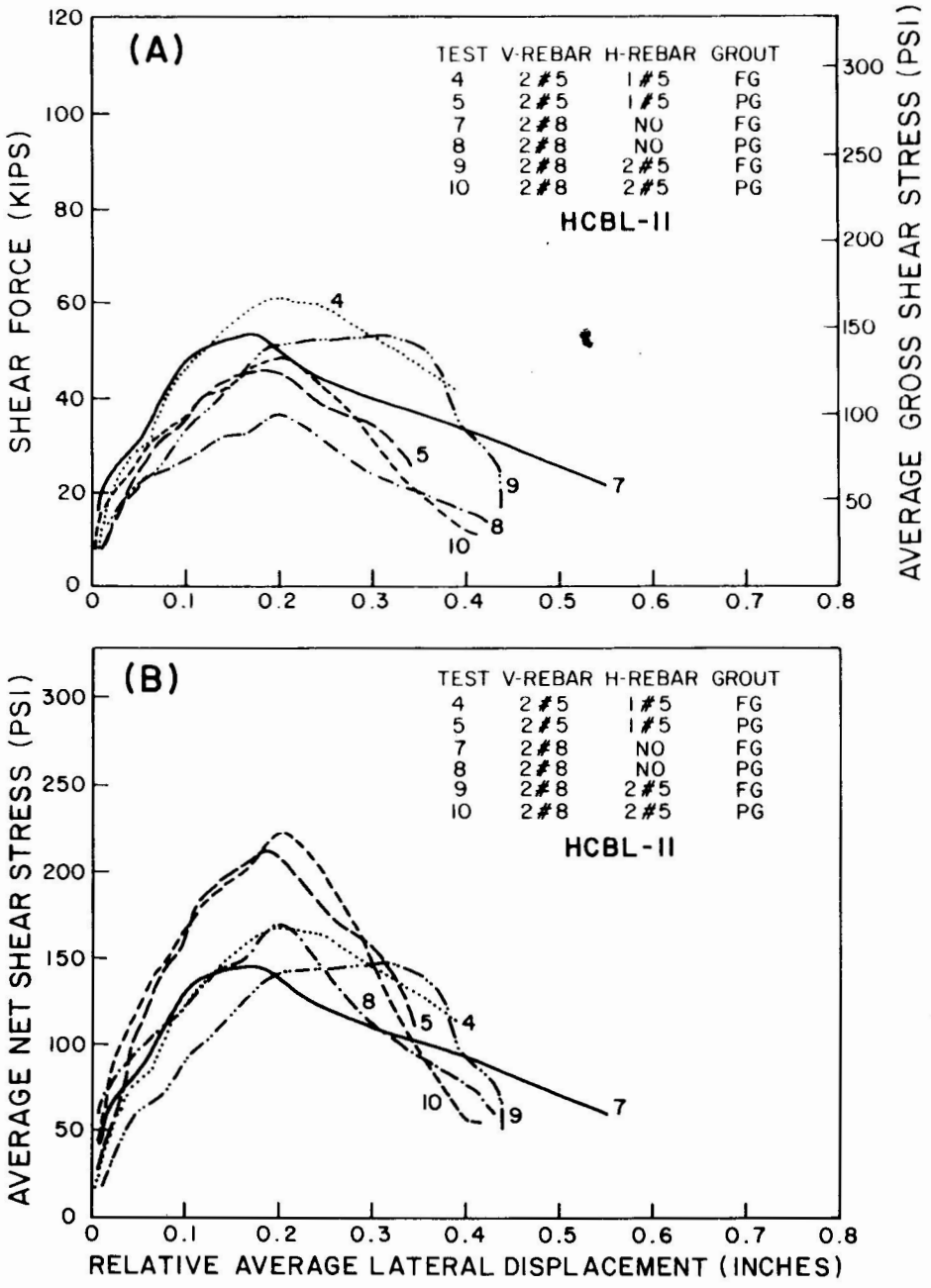

FIGURE 8. EFFECT OF PARTIAL GROUTING ON HYSTERESIS ENVELOPE (HCBL-11)